Supplementary information

Enhanced Performance of All-Solid-State Rechargeable Air Batteries with Redox-Active Naphthoquinone-Based Polymer Electrode

Lin Guo[a], Kenji Miyatake*[a,b,c], Fang Xian[a], Fanghua Liu[a], Ahmed Mohamed Ahmed Mahmoud[a], Vikrant Yadav[a], Chun Yik Wong[a]

[a]Clean Energy Research Center, University of Yamanashi, Kofu, Yamanashi 400-8510, Japan.

[b]Hydrogen and Fuel Cell Nanomaterials Center, University of Yamanashi, Kofu, Yamanashi 400-8510, Japan

[c]Department of Applied Chemistry, Waseda University, Tokyo 169-8555, Japan.

*Corresponding author

E-mail address: miyatake@yamanashi.ac.jp (Kenji Miyatake)

Experimental section

Materials

Platinum/carbon black (Pt/CB; Pt = 47 wt.%, TEC10EA50E) and Ketjen black® (EC600JD) were purchased from Tanaka Precious Metals Co. (Tokyo, Japan). Nafion™ dispersion (ion-exchange capacity (IEC) = 0.95–1.03 meq g^{-1}, D-521; DuPont) and Nafion 212 membrane were purchased from the Chemours Company (Wilmington, DE, USA). Bis(1,5-cyclooctadiene)nickel(0) ($Ni(cod)_2$), 2,2′-bipyridine (BPY), hydrochloric acid (37.0 wt%), anhydrous toluene, dehydrated DMSO, deuterated DMSO (DMSO-d_6), DMF, sulfuric acid, potassium carbonate (K_2CO_3), 2-propanol, glacial acetic acid, 4-dichlorophenylboronic acid, 1,4-dioxane, ethyl acetate, hexane, magnesium sulfate ($MgSO_4$), sodium bisulfite ($NaHSO_3$), deuterated chloroform ($CDCl_3$), and ethanol were purchased from Kanto Chemical Co. (Tokyo, Japan) and used as received. NQ, liquid bromine, and tetrakis(triphenylphosphine)palladium(0) ($Pd(PPh_3)_4$) were purchased from TCI Co., Ltd. (Tokyo, Japan).

Methods

A ca. 60 μm-thick sulfonated polyphenylene membrane (SPP-QP) with a target IEC of 3.1 mmol g^{-1} was synthesized as previously described.[1] The 2,3-dibromonaphthalene-1,4-dione (DBNQ) monomer was prepared as previously described, with some modifications.[2] The 2,3-bis(4-chlorophenyl)naphthalene-1,4-dione (DPNQ) monomer was synthesized via Pd(0)-catalyzed Suzuki–Miyaura coupling, while the PPNQ polymer was obtained through Ni(0)-mediated polycondensation of the DPNQ monomer.

Synthesis of DBNQ. Liquid bromine (6.50 mL, 126 mmol, 2 equiv.) was added dropwise to a solution of NQ (10.00 g, 63 mmol) in glacial acetic acid. The resulting solution was stirred at room temperature for 30 min and then heated at 110°C. After reaction at this temperature for 8 h, the mixture was poured into 250 mL of ice water. The precipitate was filtered and washed with water, recrystallized from ethanol, and dried under vacuum. The pure product was obtained as a yellow solid (18.20 g, 91% yield).

Synthesis of DPNQ monomer. $Pd(PPh_3)_4$ (1.17 g, 1.01 mmol) was added to a stirred solution of DBNQ (8.00 g, 25.32 mmol), K_2CO_3 (10.50 g, 60.77 mmol), and 4-dichlorophenylboronic acid (8.71 g, 55.71 mmol) in 1,4-dioxane (160 mL) and water (40 mL). The reaction mixture was heated at 75°C for 1 h, and progression of the reaction was monitored via thin layer chromatography. After complete consumption of the starting material, the mixture was cooled to r.t., diluted with water, and extracted several times with ethyl acetate. The combined organic layer was successively washed three times with aqueous $NaHSO_3$ solution and brine, respectively, dried over $MgSO_4$, and concentrated under vacuum. The crude product was purified by column chromatography (hexane : ethyl acetate = 2:1) over silica gel, recrystallized from 2-propanol, and dried under vacuum. The product was obtained as yellow needle-like crystals (5.00 g, 52% yield).

Synthesis of PPNQ polymer. A 100 mL three-necked flask equipped with a condenser, N_2 inlet/outlet, and magnetic stirring bar was charged with DPNQ (0.49 g, 1.30 mmol), K_2CO_3 (0.20 g, 1.30 mmol), BPY(0.43 g, 2.72 mmol), and dehydrated DMSO (14 mL). The mixture was heated at 80°C, followed by the addition of $Ni(cod)_2$ (0.71 g, 2.59 mmol, 1.0 equiv. chlorine groups). After reaction at this temperature for 3 h, the mixture was poured into a large excess of hydrochloric acid. The precipitate was washed once with hydrochloric acid (8 h) and three times with pure water (2 h each). After drying in a vacuum oven overnight at 60°C, PPNQ was obtained as a reddish-brown polymer (0.47 g, 97% yield).

Preparation of positive electrode (oxygen electrode) catalyst paste. Commercial Pt/CB catalyst (0.50 g), 5 wt.% Nafion^{TM} dispersion (3.52 g), deionized water (2.07 g), and ethanol (4.06 g) were mixed using 20 zirconia balls (⌀5 mm) in a planetary ball mill (Pulverisette 6; Fritsch Milling & Sizing Inc., Pittsboro, NC, USA) at 270 rpm for 30 min, followed by rolling pot-mixing overnight. The mass ratio of Nafion^{TM} ionomer to carbon support (I/C) was adjusted to 0.70.

Preparation of negative electrode (redox-active electrode) catalyst paste. PPNQ (0.08 g in 3.70 g DMF) solution, Ketjen black® (0.30 g), 5 wt.% Nafion™ dispersion (9.60 g), and ethanol (3.70 g) were mixed using 20 zirconia balls (⌀5 mm) in a planetary ball mill at 270 rpm for 30 min, followed by rolling pot-mixing overnight. I/C was adjusted to 2.0, and the mass ratio of PPNQ: Ketjen black® :Nafion™ binder was 10:30:60.

Preparation of CCM. The positive and negative electrode pastes were sprayed on either side of the SPP-QP membrane using a power-pulse swirl-spray machine (nozzle type: A7A for Swirl ver. 3, dual syringe, type 2; Nordson Corp., Westlake, OH, USA). The resulting CCM was dried overnight at 60°C and hot-pressed at 140°C and 10 kgf cm^{-2} for 3 min. The geometric area of both sides of the electrode was 4.41 cm^2 (2.1 × 2.1 cm^2). The Pt and redox-active material (PPNQ) loadings in the positive and negative electrodes were 0.50 ± 0.05 and 1.00 ± 0.05 mg cm^{-2}, respectively.

Cell fabrication. A 280 µm-thick gas diffusion layer (GDL) (titanium with platinum plating, 2GDL07N-030 BS02PT; Bekaert Toko Metal Fiber Co., Ltd., Ibaraki, Japan) and one or two 100 or 200 µm-thick gaskets (silicon rubber–polyethylene naphthalate–silicon rubber; Maxell Kureha Co., Ltd., Osaka, Japan) were placed on the positive electrode side. A 215 µm-thick GDL (22BB; SGL Carbon Group Co., Ltd., Wiesbaden, Germany) and two gaskets (same as those used for the positive electrode side) were placed on the negative electrode side. The CCM was mounted in a single cell, with serpentine flow channels on the Pt-plated Ti and carbon separators for the positive and negative electrodes, respectively. A reference electrode (reversible hydrogen electrode fabricated using Pt/C attached to a gold wire) was attached to one side of the membrane through the GDL (22BB).

Proton conductivity measurement. The in-plane impedance (R) of the membranes was measured with a solid electrolyte analyzer system (MSBAD-V-FC, Bel Japan Co.) in a temperature/humidity-controllable chamber. The R value was measured using a four-probe conductivity cell equipped with an AC impedance analyzer (Solartron 1255B and 1287, Solartron Inc.). After equilibrating at a given humidity , the R value was recorded as impedance plots in the frequency range from 10^5 to 1 Hz with an AC amplitude of 300 mV and a DC bias of 0 V. The in-plane proton conductivity (σ) of the membranes was calculated from the following equation: $\sigma = L/(A \times R)$, where L and A are the distance between the two reference electrodes and the cross-sectional area, respectively.

Electrochemical Impedance Spectroscopy (EIS) measurement. The EIS of SSAB was tested from 5,000 to 0.01 Hz at 0.1 A with supplying H_2 (100 mL min^{-1}) and N_2 (100 mL min^{-1}) to the positive and the negative electrodes, respectively, at 40 ºC and 80% relative humidity (RH).

Micromorphology. Scanning electron microscopy (SEM) images were obtained using a Hitachi SU3500 equipped with an EDS detector (Oxford Instruments) at an accelerating voltage of 5 kV.

Operation and evaluation of SSABs. The SSABs were operated at 40°C, with the supplied gases humidified at 80% or 100% RH. The general operating procedures for the charging/discharging cycle and rate characteristic tests are listed in Tables S1 and S2, respectively. For the charge/discharge cycling test at 15 C, the measurements were manually paused at every 20 cycles due to the long testing duration. At each pause, both the negative and the positive electrodes were purged with nitrogen overnight (ca. 12 h). Testing was resumed on the following day under the identical conditions without any changes in the cell configuration.

Cyclic voltammograms (CV) measurement. In the SSAB configuration, the CV measurement was performed using a three-electrode setup, with the negative electrode serving as the working electrode, and the positive electrode acting as both the counter and reference electrodes. N_2 and H_2 were respectively supplied to the negative and positive electrodes. The CV was recorded at a scan rate of 20 mV s^{-1}. For the CV measurement in a liquid electrolyte, the catalyst ink of the negative electrode (identical to that used in CCM preparation) was drop-cast onto a glassy carbon rotating disk electrode (RDE, 5 mm in diameter, Meiden Hokuto Co., Japan) as the working electrode, maintaining a redox-active material loading of 1 mg cm^{-2}. A platinum mesh and a reversible hydrogen electrode (RHE) were used as the counter and reference electrodes, respectively. The electrochemical measurements were carried out using a potentiostat (HZ-5000, Meiden Hokuto Co., Japan) and a rotation control system (HR301, Meiden Hokuto Co., Japan) in 0.05 M sulfuric acid. CV was measured in N_2-saturated solution at a scan rate of 20 mV s^{-1} and a rotation speed of 3000 rpm.

Table S1. Procedure of charge/discharge cycle test.

Step	Operation time (min)	Supplied gas and the flow rate (mL min^{-1})						Rate (C)	Remarks
		Negative electrode		Positive electrode		Reference electrode			
1	overnight	N_2	100	N_2	100	H_2	slight	0	-
2	(charging)							15	Till the negative electrode reached 0 V
3	5			air	476			0	-
4	(discharging)							15	Till the cell voltage became 0 V
5	1			N_2	100			0	-
Repeat steps from 2 to 5.									

Table S2. Procedure of rate characteristic test.

Step	Operation time (min)	Supplied gas and the flow rate (mL min^{-1})						Rate (C)	Remarks
		Negative electrode		Positive electrode		Reference electrode			
1	overnight	N_2	100	N_2	100	H_2	slight	0	-
2	(charging)							4	Till the negative electrode reached 0 V
3	5			air	476			0	-
4	(discharging)							4 10 20 40 60 80 100	Till the cell voltage became 0 V
5	1			N_2	100			0	-

Table S3. SSAB performance of PPNQ and NQ.

a: the data of NQ was obtained at 100% RH in SSAB.

	PPNQ	NQ [a]
Redox active material utilization (%)	17	16.5
OCV (V)	0.73	1.10
Nominal cell voltage (V) at discharging	0.55–0.45	0.40–0.24
Discharge capacity retention (%) at 100 C	84	79
Initial discharge capacity (mAh g^{-1})	58.7	81.7
Discharge capacity retention (%) after 100 charge/discharge cycles at 15 C	98	90

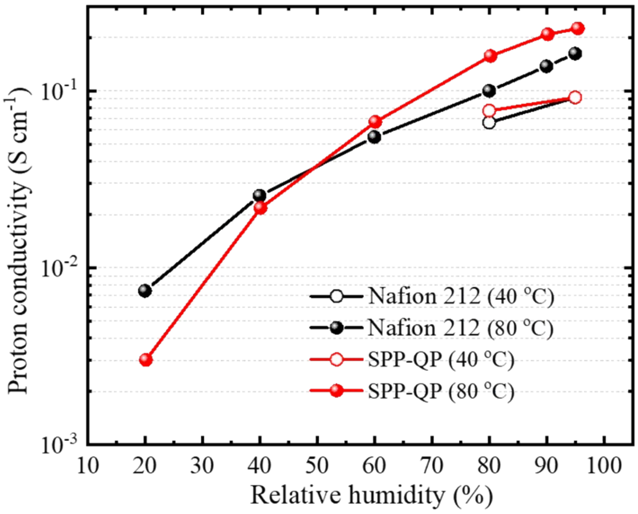

Figure S1. Proton conductivity of SPP-QP membrane at 40 and 80 ^{o}C (data of Nafion 212 membrane is included for comparison).

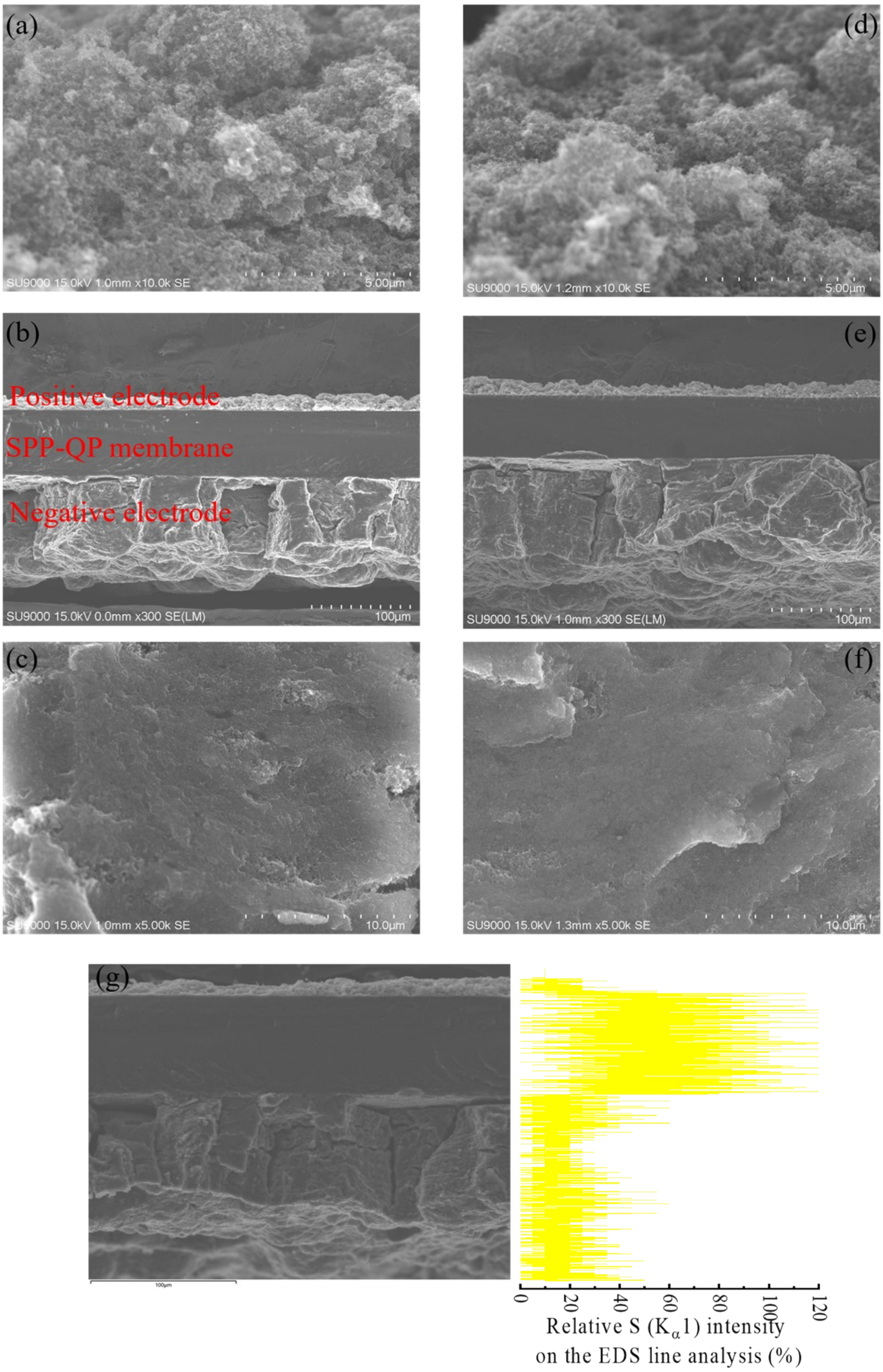

Figure S2. Cross-sectional SEM images of the positive electrode (a, d), the overall CCM (b, e), and the negative electrode (c, f) for the fresh (left) and aged (right) samples. (g) Relative sulfur (S Kα1) intensity obtained from the EDS line analysis.

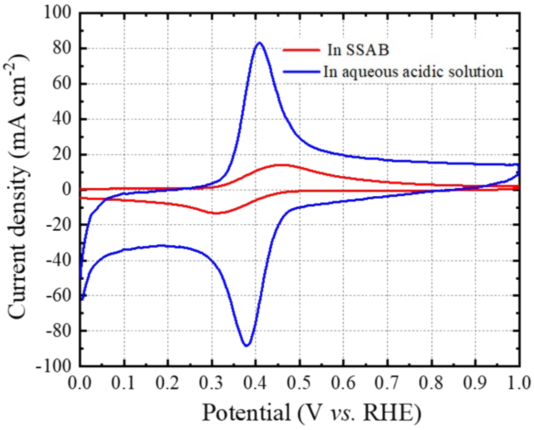

Figure S3. CV curve (red line) of the SSAB-PPNQ cell at a scan rate of 20 mV s^{-1} (40 °C, 80% RH) for the negative electrode, and CV curve (blue line) of the PPNQ-modified electrode in 0.05 M sulfuric acid under nitrogen at a scan rate of 20 mV s^{-1}.

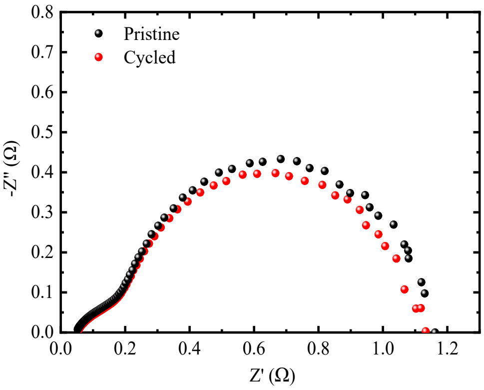

Figure S4. Nyquist plot of pristine and cycled SSAB-PPNQ.

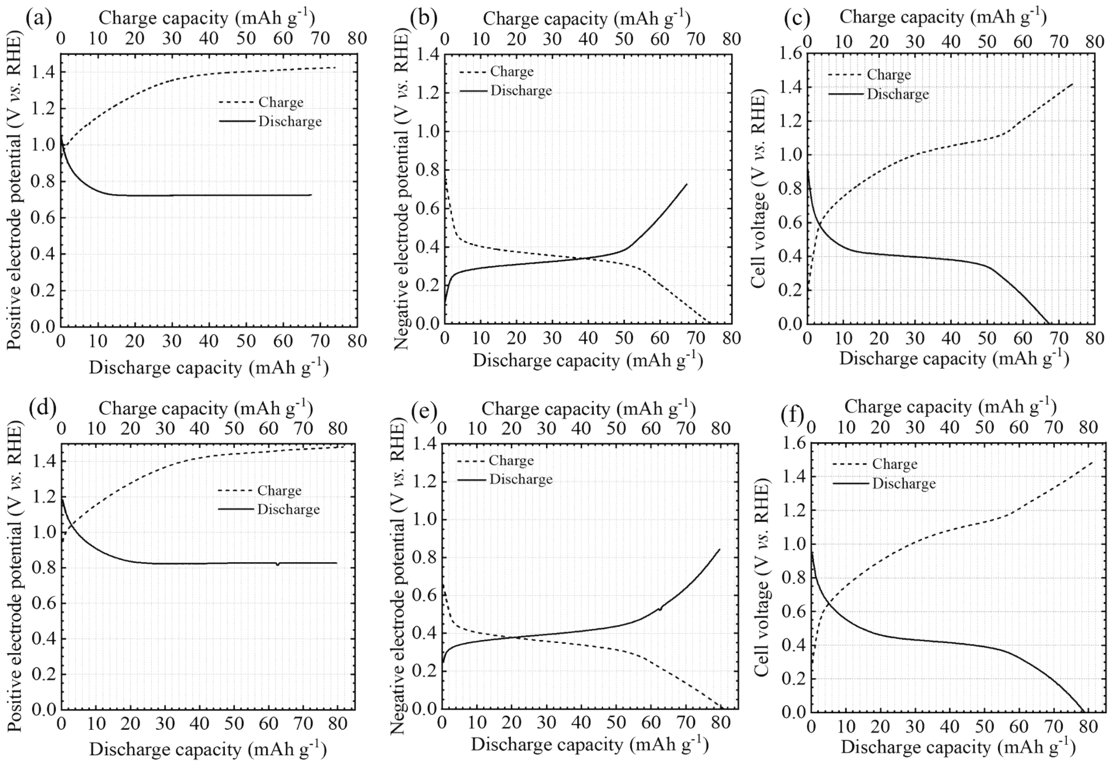

Figure S5. Charge and discharge curves measured at a current density of of 0.06 mA cm^{-2} (1 C, top) and 0.03 mA cm^{-2} (0.5 C, bottom): (a, d) positive electrode potential, (b, e) negative electrode potential and (c, f) cell voltage.

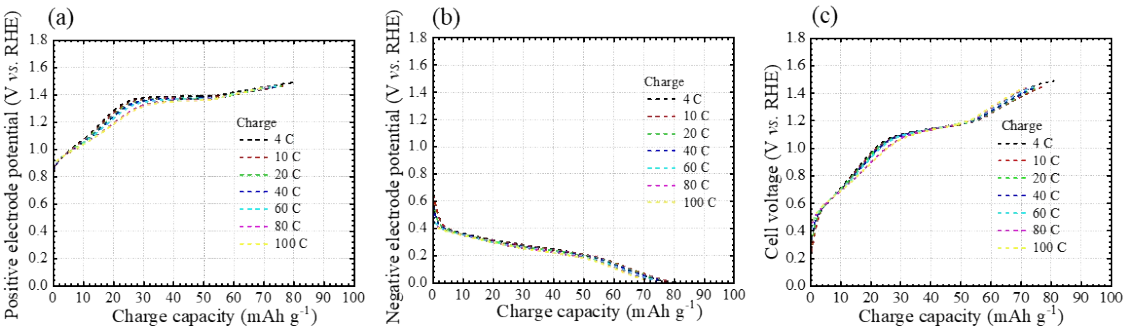

Figure S6. Charging curves of (a) positive electrode potential, (b) negative electrode potential, (c) cell voltage, and (d) Coulombic efficiency measured at 4, 10, 20, 40, 60, 80, and 100 C rates (or current densities of 0.24, 0.59, 1.17, 2.35, 3.53, 4.70 and 5.87 mA cm^{-2}).

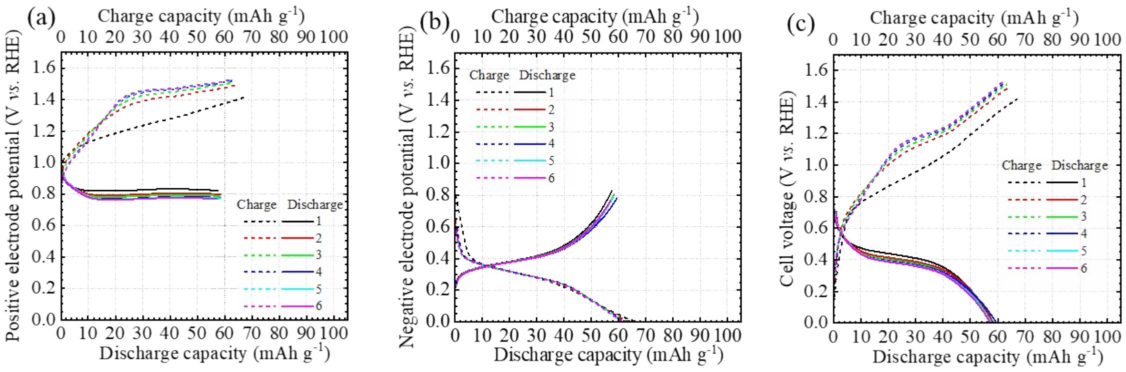

Figure S7. Charging/discharging curves of the SSAB-PPNQ cell measured from the 1st to the 6th cycle at 0.88 mA cm^{-2} (15 C rate): (a) positive electrode potential, (b) negative electrode potential and (c) cell voltage.

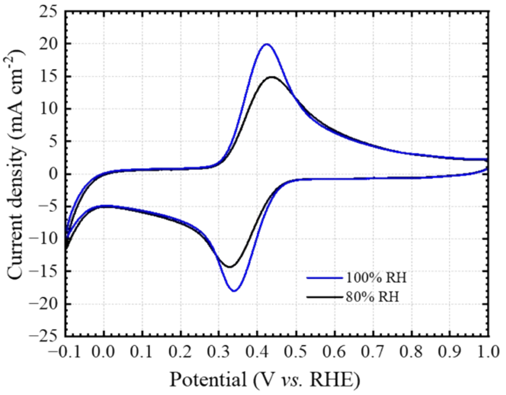

Figure S8. CV curves scanned at 20 mV s^{-1} for cycled negative electrodes at 80% and 100% RH.

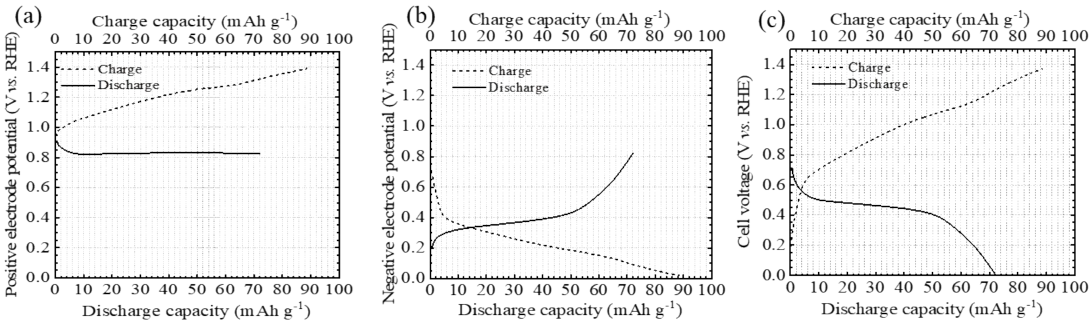

Figure S9. Charging/discharging curves measured at 100% RH and a current density of 0.23 mA cm^{-2} (3.4 C rate) after cycling at 80% RH for 100 cycles: (a) positive electrode potential, (b) negative electrode potential and (c) cell voltage.

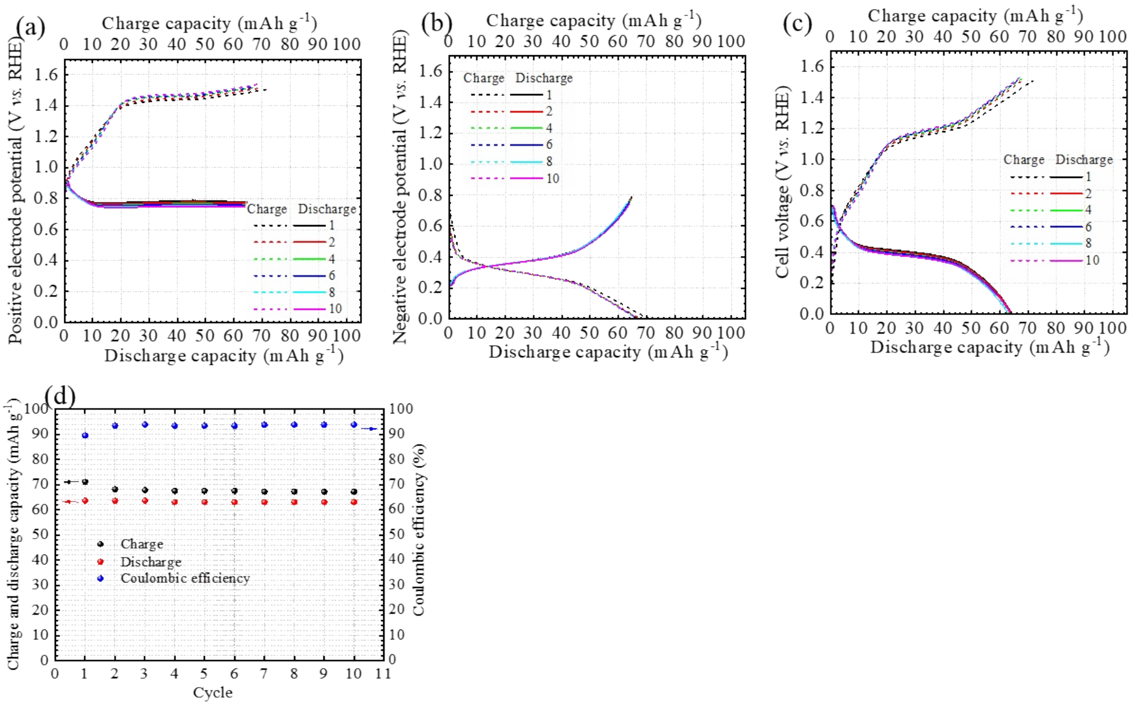

Figure S10. Charging and discharging curves measured for 10 cycles at 100% RH and a current density of 1.02 mA cm^{-2} (15 C rate) after 100 cycles at 80% RH: (a) positive electrode potential, (b) and negative electrode potential (c) cell voltage. Changes in (d) charge/discharge capacities and Coulombic efficiencies during cycling.

References

1. J. Miyake, R. Taki, T. Mochizuki, R. Shimizu, R. Akiyama, M. Uchida and K. Miyatake, *Sci. Adv.* 2017, **3**, eaao0476.
2. Y. Jia, Y. Xu, R. Nie, F. Chen, Z. Zhu, J. Wang and H. Jing, *J. Mater. Chem. A*, 2017, **5**, 5495–5501.